J Biosci Vol. 43, No. 1, March 2018, pp. 139–148
DOI: 10.1007/s12038-017-9726-1

Tetrahymena dynamin-related protein 6 self-assembles independent of membrane association

Usha P Kar, Himani Dey and Abdur Rahaman*

School of Biological Sciences, National Institute of Science Education and Research-HBNI, Bhubaneswar, India

**Corresponding author (Email, arahaman@niser.ac.in)*

MS received 9 October 2017; accepted 28 November 2017; published online 30 December 2017

Self-assembly on target membranes is one of the important properties of all dynamin family proteins. Drp6, a dynamin-related protein in *Tetrahymena,* controls nuclear remodelling and undergoes cycles of assembly/disassembly on the nuclear envelope. To elucidate the mechanism of Drp6 function, we have characterized its biochemical and biophysical properties using size exclusion chromatography, chemical cross-linking and electron microscopy. The results demonstrate that Drp6 readily forms high-molecular-weight self-assembled structures as determined by size exclusion chromatography and chemical cross-linking. Negative stain electron microscopy revealed that Drp6 assembles into rings and spirals at physiological ionic strength. We have also shown that the recombinant Drp6 expressed in bacteria is catalytically active and its GTPase activity is not enhanced by low salt. These results suggest that, in contrast to dynamins but similar to MxA, Drp6 self-assembles in the absence of membrane templates, and its GTPase activity is not affected by ionic strength of the buffer. We discuss the self-assembly structure of Drp6 and explain the basis for lack of membrane-stimulated GTPase activity.

Keywords. Drp6; dynamin; GTPase activity; membrane remodelling; self-assembly; *Tetrahymena*

1. Introduction

The *Tetrahymena* dynamin-related protein 6 (Drp6) localizes to the nuclear envelope and plays a role in nuclear remodelling in a stage-specific manner (Rahaman *et al.* 2008). Its function is essential during nuclear differentiation where the germline micronuclei undergo several-fold expansion to form somatic macronuclei (Rahaman *et al.* 2008). Drp6 is a member of a family of large GTPase proteins that include classical dynamins and dynamin-related proteins (DRPs). Members of this family perform several important cellular functions such as endocytosis, cytokinesis, maintenance of mitochondrial dynamics and antiviral activity (Praefcke and McMahon 2004; Kar *et al.* 2017). They are mechano-chemical enzymes that couple the free energy of GTP hydrolysis with membrane remodelling. Classical dynamins are involved in membrane trafficking during endocytic vesicle scission at the plasma membrane and secretory vesicle scission at Golgi (Praefcke and McMahon 2004; Kar *et al.* 2017). Mitochondrial DRPs are involved in maintenance of mitochondrial dynamics by mediating both fission and fusion (Chan 2006; Chang and Blackstone 2010). While fission DRPs like Drp1/Dnm1/Dlp1 oligomerize on mitochondrial fission sites and bring about fission, fusion DRPs such as Mfn1/Mfn2/Fzo1 and Mgm1/OPA1 mediate fusion of outer and inner mitochondrial membranes, respectively (van der Bliek *et al.* 2013). A group of interferon-induced DRPs such as MxA and MxB exhibit antiviral activity against a wide range of viruses by forming complexes around the viral nucleoproteins, different from the canonical membrane remodelling function (Haller *et al.* 2007; Haller and Kochs 2011). Dynamins and DRPs are multi-domain proteins, and share similar domain architecture. Classical dynamins harbour five functionally distinct domains: a GTPase domain, middle domain (MD), GTPase effector domain (GED), pleckstrin homology (PH) domain, and proline-rich domain (PRD) (figure 1A) (Hinshaw 2000; Praefcke and McMahon 2004). Dynamin-related proteins retain three characteristic domains but lack PRD (involved in protein-protein interactions) and the PH domain (responsible for membrane binding). Although DRPs lack a defined PH domain, an exposed lipid binding loop in MxA, an alpha helical membrane penetrating paddle domain in BDLP and trans-membrane helices in Mitofusins, OPA1, Mgm1 and atlastins function as membrane binding motifs (Hermann

Electronic supplementary material: The online version of this article (https://doi.org/10.1007/s12038-017-9726-1) contains supplementary material, which is available to authorized users.

et al. 1998; Fritz *et al.* 2001; Sesaki *et al.* 2003; Low *et al.* 2009; Moss *et al.* 2011; Von Der Malsburg *et al.* 2011).

Although involved in diverse functions, the members of this family share common biochemical properties such as low-affinity GTP binding, a high propensity to oligomerize around lipid templates, and oligomerization-stimulated GTP hydrolysis (Antonny *et al.* 2016). A characteristic feature of dynamin family proteins is their ability to polymerize into regular structures on membrane templates. Dynamin self-assembles into rings or helices around microtubules or the neck of clathrin-coated vesicles (Hinshaw and Schmid 1995; Takei *et al.* 1995). Other DRPs such as MxA, Dnm1, OPA1 and BDLP also form rings and helical oligomers on their target (Low *et al.* 2009; Tadato *et al.* 2010; Mears *et al.* 2011; Von Der Malsburg *et al.* 2011).

The intra- and inter-molecular interactions that promote self-assembly of dynamins into higher-order rings and filamentous structures stimulate GTP hydrolysis, and are important for membrane-remodelling functions (Praefcke and McMahon 2004; Antonny *et al.* 2016). Cycles of assembly and disassembly of dynamin oligomers at sites of endocytosis are important for vesicle scission. This cycle of assembly/disassembly is important for functions of other DRPs as well, for example, Drp1 during mitochondrial fission, mitofusins/Mgm1/OPA1/Fzo1 during mitochondrial fusion and MxA in antiviral activity (Sweitzer and Hinshaw 1998; Chen *et al.* 2004; Praefcke and McMahon 2004; Song *et al.* 2004; Von Der Malsburg *et al.* 2011). Disruption of assembly by mutations interfering with oligomerization results in functional inhibition of dynamins and DRPs (Song *et al.* 2004; Chang *et al.* 2010; Gao *et al.* 2010).

Although the role of Drp6 in *Tetrahymena* macronuclear development has been established, the mechanism of its function is not known. Like other DRPs, Drp6 also harbours three domains – the G domain, MD and GED (figure 1A) (Rahaman *et al.* 2008). In an attempt to understand the mechanism of Drp6 function, we evaluated its GTPase activity and oligomeric state. Here we demonstrate that Drp6 forms regular higher-order assembled structures including rings and helical spirals, and has an intrinsic GTP hydrolysis rate comparable to that of classical dynamin. Interestingly, our results suggest that unlike dynamin and other DRPs, Drp6 assembly is independent of membrane association.

2. Materials and methods

2.1 *Cloning, expression and purification of recombinant Drp6*

The codon optimized *DRP6* gene was synthesized (Eurofins, MWG) and obtained in the pUC57 vector. The insert was released and cloned into the pRSETB expression vector (a kind gift from Prof MS Shaila, IISc, Bangalore) using KpnI and EcoRI sites. The pRESTB-*DRP6* construct was transformed into BL21 (DE3), C41 (DE3) and C43 (DE3) strains of *E. coli* to express the protein bearing an N-terminal His_6 tag. The expression of Drp6 was optimized by inducing the transformants for 5 h at 37 °C and 16 h at 18 °C. Maximum expression was obtained in C41 cells when induced with 0.5 mM IPTG (isopropyl β-D-1-thiogalactopyranoside) (MP biomedical) at 18 °C. The human dynamin 1 in pET15B (a kind gift from Prof Mark A Lemmon, University of Pennsylvania, USA) was expressed in *E. coli* rosetta (DE3). For large-scale expression, 6 mL of overnight grown culture from single colony was inoculated into 1 L LB broth

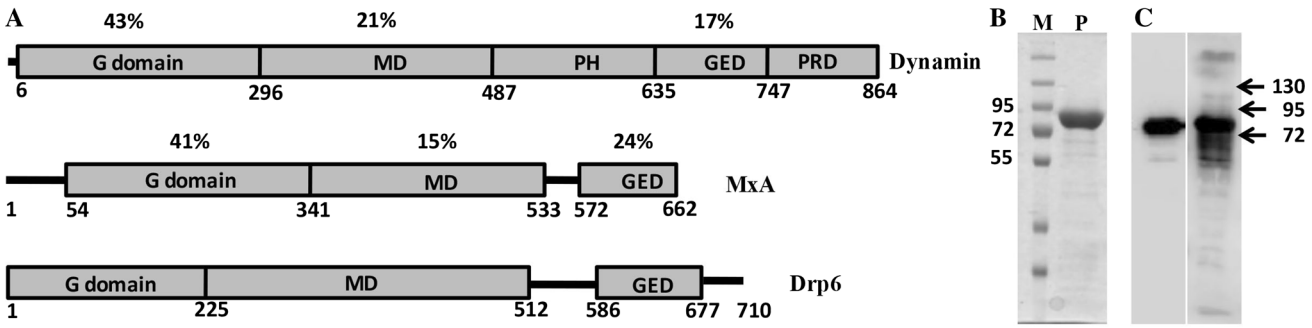

Figure 1. Domain structure and purification of recombinant Drp6. (**A**) Schematic representation of domains of dynamin 1, MxA and Drp6. Dynamins contain five distinct domains indicated as G domain, MD, PH domain, GED and PRD. MxA and Drp6 retain three core domains but lack PH domain and PRD. The numbers represent the position of amino acids in the proteins and % represents percentage identity of corresponding domains with Drp6. (**B**) SDS-PAGE analysis of purified Drp6. Drp6 expressed in *E. coli* C41 strain was purified using Ni-NTA column, separated on a 10% SDS PAGE gel and visualized after Coomassie staining. M and P denotes molecular weight standards and purified protein respectively. (**C**) Western blot analysis of purified Drp6 using anti-histidine antibody (left panel) and anti-Drp6 antibody (right panel). Two independent blots were used for probing with two different antibodies, i.e. anti-histidine antibody and anti-Drp6 antibody. The molecular weight markers are indicated on the side by arrows. Details of anti-Drp6 antibody is described in supplementary information (supplementary figure 6).

supplemented with 100 μg/mL ampicillin and grown at 37 °C at 220 r.p.m. until the OD_{600} reached 0.4–0.5. The culture was shifted to 18 °C, 0.5 mM IPTG was added after 1 h and protein expression was induced for 16 h at the same temperature.

For protein purification, cell pellets were re-suspended in 50 mL of ice cold buffer containing 25 mM HEPES pH 7.5, 300 mM NaCl, 2 mM $MgCl_2$, 2 mM β-mercaptoethanol and 10% glycerol (buffer A) supplemented with EDTA-free protease inhibitor cocktail (Roche) and 100 mM phenylmethyl sulfonyl fluoride (PMSF, Sigma). The cells were ruptured by sonication and the crude lysate was centrifuged at 15,000 r.p.m (24,652*g*) followed by centrifugation at 30,000 r.p.m (104,350*g*) in 45 Ti rotor (Beckman) for 45 min at 4 °C. The supernatant was incubated with pre-equilibrated Ni-NTA resin (Qiagen) for 2 h, the resin was washed with 100 bed volume buffer A supplemented with 50 mM imidazole and the protein was eluted with 250 mM imidazole in the same buffer. The purified protein was checked by Coomassie-stained SDS-PAGE gels and the purity was assessed by Image J analysis (NIH). The fractions containing the purified protein were pooled, dialysed with buffer A to get rid of imidazole and concentrated using Amicon ultra-15 centrifugal filters (Millipore) with a molecular cut-off of 10 kDa. The purified protein was confirmed by Western blot analysis using anti-Drp6 polyclonal antibody (1:500) and anti-His monoclonal antibody (Sigma) (1:5000). Details showing specificity of anti-Drp6 polyclonal antibody is described in supplementary information (supplementary figure 1). Concentration of purified proteins were determined by Bradford assay (BioRad).

2.2 *Size exclusion chromatography*

For size exclusion chromatography, 500 μL of concentrated recombinant Drp6 or human dynamin 1 (0.5 mg/mL) was loaded onto a Superdex 200 GL 10/300 (GE Life Sciences) pre-equilibrated with buffer A without glycerol. The column was run at a flow rate of 0.5 mL/min and 0.5 mL fractions were collected. The column was calibrated by using standard molecular weight markers from Sigma. The peak fractions were checked on SDS-PAGE followed by silver staining.

2.3 *Chemical cross-linking*

Cross-linking of recombinant Drp6 was performed using bis(sulfosuccinimidyl)suberate (BS^3, Pierce, Thermo Scientific) in buffer containing 25 mM HEPES pH 7.5, 150 mM NaCl and 2 mM $MgCl_2$ (Buffer B) (Muhlberg 1997). The protein (2 μM) was incubated in presence of 0.5 mM or 1 mM BS^3 at room temperature for 5 min to 30 min. The reactions were stopped by adding glycine to 100 mM and the cross-linked products were analysed on 6% SDS-PAGE followed by silver staining.

2.4 *Negative stain electron microscopy*

Purified recombinant Drp6 (1 μM) in buffer B was incubated with or without 0.5 mM GTPγS (Sigma) in a 20 μL reaction volume for 20 min at room temperature and was adsorbed for 5 min onto a 200 mesh carbon coated Copper grid (Ted Pella, Inc.). The grid was stained with a drop of 2% freshly prepared uranyl acetate (MP Biomedical) for 2 min followed by washing with another drop of 2% uranyl acetate for 6 s (Hinshaw and Schmid 1995). The grid was dried at room temperature for 10 min and observed on a FEI Tecnai G2 120 kV electron microscope.

2.5 *Measurement of GTP hydrolysis activity*

The GTP hydrolysis activity of recombinant Drp6 and human dynamin 1 was measured by colorimetric assay using a Malachite Green-based phosphate assay kit (BIOMOL Green, Enzo Life Sciences). Typically, a 90 μL reaction volume containing 1 μM Drp6 or 0.5 μM human dynamin 1 and 1 mM GTP (Sigma) in buffer B was incubated at 37 °C. Aliquots of 20 μL were collected at different time intervals and the reactions were stopped by adding 5 μL of 0.5 mM EDTA. To this, 1 mL BIOMOL green solution was added and the colour was allowed to develop for 20 min at room temperature before measuring the absorbance at 620 nm. The amount of phosphate released was quantified by using phosphate standards provided with the kit. To measure GTPase activity at low salt, the assay was performed under same conditions except the NaCl concentration of the buffer was kept at 40 mM. For measuring K_m and K_{cat}, reactions were performed in triplicate with varying GTP concentrations ranging from 50 μM to 2000 μM for 10 min at 37 °C using 2 μM Drp6. Three independent assays were performed for each batch of purified protein and data are presented from three batches of purified proteins. The values were plotted and analysed using Origin Pro8.0 program. One-way ANOVA (non-parametric Kruskal–Wallis test) was used to assess statistical significance between different experiments.

3. Results

3.1 *Expression and purification of recombinant Drp6*

In order to understand the structure and function of Drp6, we expressed Drp6 in *E. coli* C41 (DE3) cells and purified soluble Drp6 bearing an N-terminal His_6 tag. The growth at low temperature was used for optimal expression of the

protein to avoid formation of inclusion bodies. To eliminate membrane bound proteins, the bacterial cell lysate was subjected to ultracentrifugation and the clarified lysate was used for purification using Ni^{2+} affinity chromatography. The purified protein migrated at 87 kDa by SDS-PAGE, corresponding to its calculated molecular mass (figure 1B). The identity of the protein was further confirmed by Western blot analysis with anti-Drp6 antibody and anti-His antibody (figure 1C). The purified protein was estimated to be ∼90% pure as determined by Image J analysis. Since several attempts to purify Drp6 further by ion exchange chromatography resulted in substantial loss of the protein without significant improvement in purity, we used Ni-NTA-purified Drp6 for subsequent experiments.

3.2 *Drp6 exists as a self-assembled structure*

Classical dynamins exist as dimers and tetramers under non-assembly conditions such as high ionic strength solutions containing 150 mM NaCl or more (Warnock *et al.* 1996; Ramachandran *et al.* 2007; Kenniston and Lemmon 2010). They self-assemble into rings and spiral structures either at low ionic strength (50 mM NaCl or less) or on membrane templates at physiological ionic strength (150 mM NaCl) (Hinshaw and Schmid 1995; Carr and Hinshaw 1997; Muhlberg 1997; Sweitzer and Hinshaw 1998). Self-assembly is facilitated by membrane association and promotes enhanced GTPase activity; this is also true for DRPs including Dnm1,Dlp1, Mgm1, Mfn1 and Fzo1 (Gao *et al.* 2010; Tuma and Collins 1994; Warnock *et al.* 1996; Yoon *et al.* 2001; Zhu *et al.* 2004; Meglei and McQuibban 2009).

To ask whether Drp6 also self-assembles into larger structures, we assessed its oligomerization state by using analytical size exclusion chromatography and chemical cross-linking. In gel filtration experiments, a major fraction of purified Drp6 eluted as a high-molecular-weight species in the void volume (7.8 mL) at 300 mM NaCl (figure 2A). This suggests that Drp6 exists as an assembled complex under high salt concentration whose molecular mass exceeds 660 kDa, the exclusion limit of the gel filtration column. To exclude the possibility that self-assembly is influenced by bacterial environment, we have expressed human dynamin in bacteria, purified under same conditions, and performed gel filtration experiments. As reported previously (Kenniston and Lemmon 2010), human dynamin did not form self-assembled structure under same buffer conditions (supplementary figure 2). Moreover, similar to Drp6, another dynamin-related protein MxA, when expressed and purified in bacteria, formed self-assembled structure even at high salt concentration (Richter *et al.* 1995; Kochs *et al.* 2002). Therefore, it appears that some of the dynamin family proteins have self-assembly properties different from classical dynamin.

The oligomeric unit of dynamins are usually a dimer or a tetramer and these oligomers form the basic unit for self-assembly (Cocucci *et al.* 2014). A peak corresponding to dimer (>150 kDa) was also observed in the size exclusion chromatography (figure 2A). Therefore, it appears that the oligomeric state of Drp6 is a dimer, which forms higher-order self-assembled structures. The exact size of assembled Drp6 eluted in the void volume could not be determined by gel filtration analysis. However, since monomeric Drp6 has a molecular mass of ∼87 kDa, we infer that the assembled complex contains at least 6 monomeric subunits. It is possible that recombinant protein purified from *E. coli* is contaminated with DNA or RNA and the peak observed in the void volume is due to protein bound with nucleic acid. To exclude this possibility, we have examined the presence of nucleic acid contamination (if any) in the purified protein by measuring the ratio of A_{260}/A_{280}. A ratio of 0.8±0.05 eliminates the possibility of nucleic acid contamination in the purified protein and suggests that the protein in the void peak is due to large oligomeric species of Drp6. Since the high-ionic-strength buffer used in these experiments mimics the membrane-free state (Ramachandran *et al.* 2007), these results imply that Drp6 does not require membrane association for self-assembly, and therefore differs from other known dynamin family members. Further, mutations equivalent to R399A (R414 in Drp6) and others around this residue required for the assembly of Dynamin (Song *et al.* 2004) did not disrupt the self-assembly of Drp6. Similar to the wild-type Drp6, a major fraction of the Drp6-R414A mutant eluted as a self-assembled structure in the void volume along with a minor peak (possibly representing dimeric structure) in the gel filtration chromatography (supplementary figure 3). This suggests that the assembly interface is likely different in Drp6.

To better understand the oligomeric state of Drp6, we performed chemical cross-linking experiments using BS^3 as a cross-linker (an irreversible amine to amine cross-linker). Different concentrations of BS^3 were used to cross-link Drp6 for different time periods and the cross-linked products were separated on 6% SDS-PAGE gels. As shown in figure 2B, in addition to a band at its monomeric position (∼87 kDa), other high-molecular-weight bands are also visible around 250 kDa as well as at the top of the separating gel. We also observed very-high-molecular-weight cross-linked products in the stacking gel appearing as a smear (figure 2B). With increasing time and cross-linker concentrations, the lower-molecular-weight bands disappeared with concomitant increase in the appearance of very-high-molecular-weight species at the top of the stacking gel (shown as vertical arrow in figure 2B). Although the exact nature of the oligomeric status could not be determined, this result corroborates the presence of high-molecular-weight structures observed by size exclusion chromatography. Taken together, the above results suggest that Drp6 self-assembles into very-high-molecular-weight structures in high ionic strength buffer independent of membrane association.

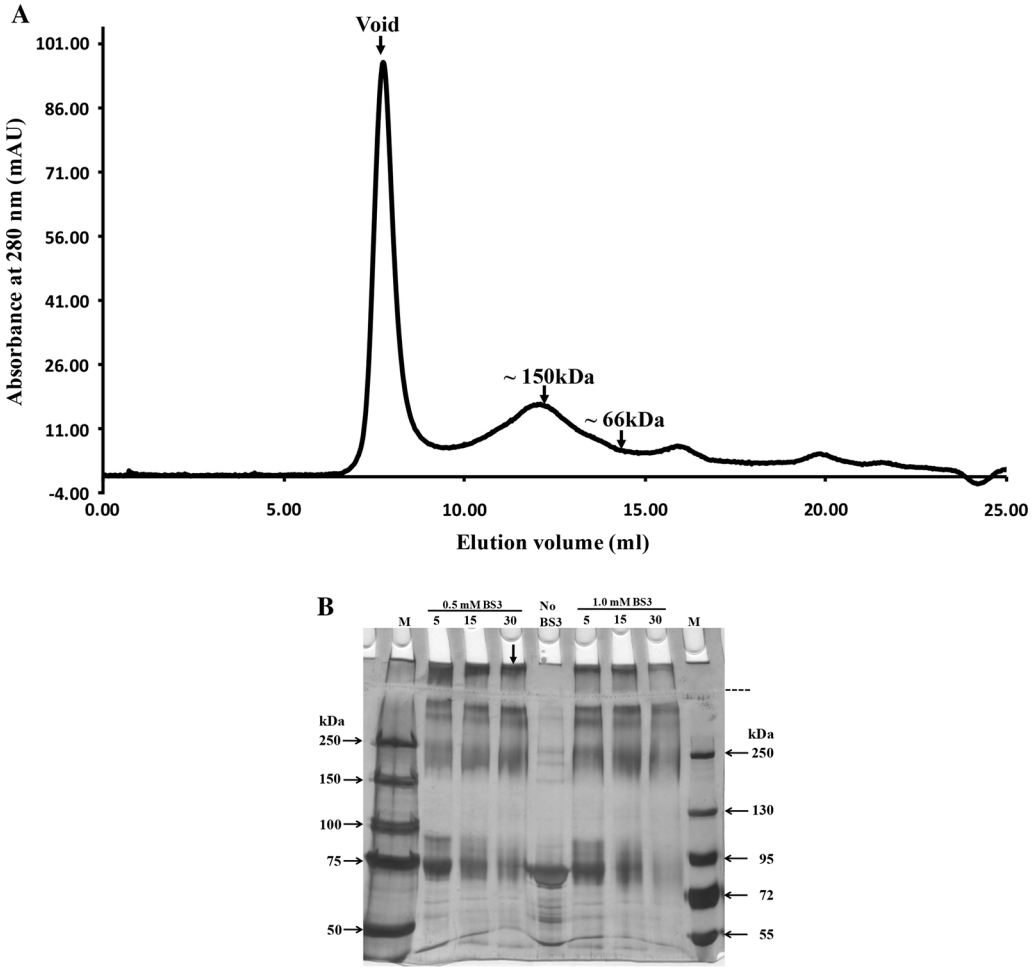

Figure 2. Drp6 self-assembles into a high-molecular-weight structure. (**A**) Size exclusion chromatography profile of Drp6. The protein was purified from cell lysate after centrifugation at ~100,000*g* to eliminate membrane-bound proteins. Purified Drp6 (0.5 mg/mL) was fractionated on a Superdex GL 10/300 column in buffer A containing 300 mM NaCl and excluding glycerol. The void peak and positions of the standard molecular weight markers are indicated in the chromatogram. A second peak around 150 kDa also contains Drp6 and may represent dimeric state. (**B**) Chemical cross-linking of Drp6 with BS^3. Silver stained 6% SDS PAGE gel showing purified Drp6 cross-linked with either 0.5 mM (left lanes) or 1.0 mM BS^3 (right lanes) for 5, 15 and 30 min. The dotted line at right denotes the interface between stacking and separating gel. The monomeric band (No BS^3) appeared at ~87 kDa as expected. Other bands in the separating gel represents cross-linked products of different protomer numbers. Cross-linked products of very high molecular weight could not enter separating gel and appeared as smear in the stacking gel (vertical arrow).

3.3 *Ultrastructure of Drp6*

A hallmark of dynamin superfamily proteins is their property to self-assemble to form rings and helical stacks of rings (Hinshaw and Schmid 1995; Carr and Hinshaw 1997; Gao *et al.* 2010; Faelber *et al.* 2011, 2012; Ford *et al.* 2011; Antonny *et al.* 2016). To find out whether the high-molecular-weight species of Drp6 are ordered assemblies, rather than amorphous aggregates, we analysed Drp6 ultrastructure by electron microscopy. Since more than 90% of the protein appeared in void volume in gel filtration column, we used the protein purified by Ni^{2+} affinity column directly for electron microscopy. Importantly, in more than 200 electron micrographs taken from protein purified in three independent batches and then negatively stained, we observed rings and helical spirals in all the micrographs examined and did not notice any disordered aggregates. Representative micrographs are shown in figure 3 and supplementary figure 4. The rings and helical spirals had varying sizes and diameters with the size of the ring-like structures ranging from 45 to 75 nm in diameter (figure 3). The appearance of these ring structures resembles that of structures formed by dynamin family members such as classical dynamin, MxA and Dlp1 (Hinshaw and Schmid 1995; Yoon *et al.* 2001; Von Der Malsburg *et al.* 2011). The helical spirals varied in length and are generally of 60 nm diameter (figure 3). Although the

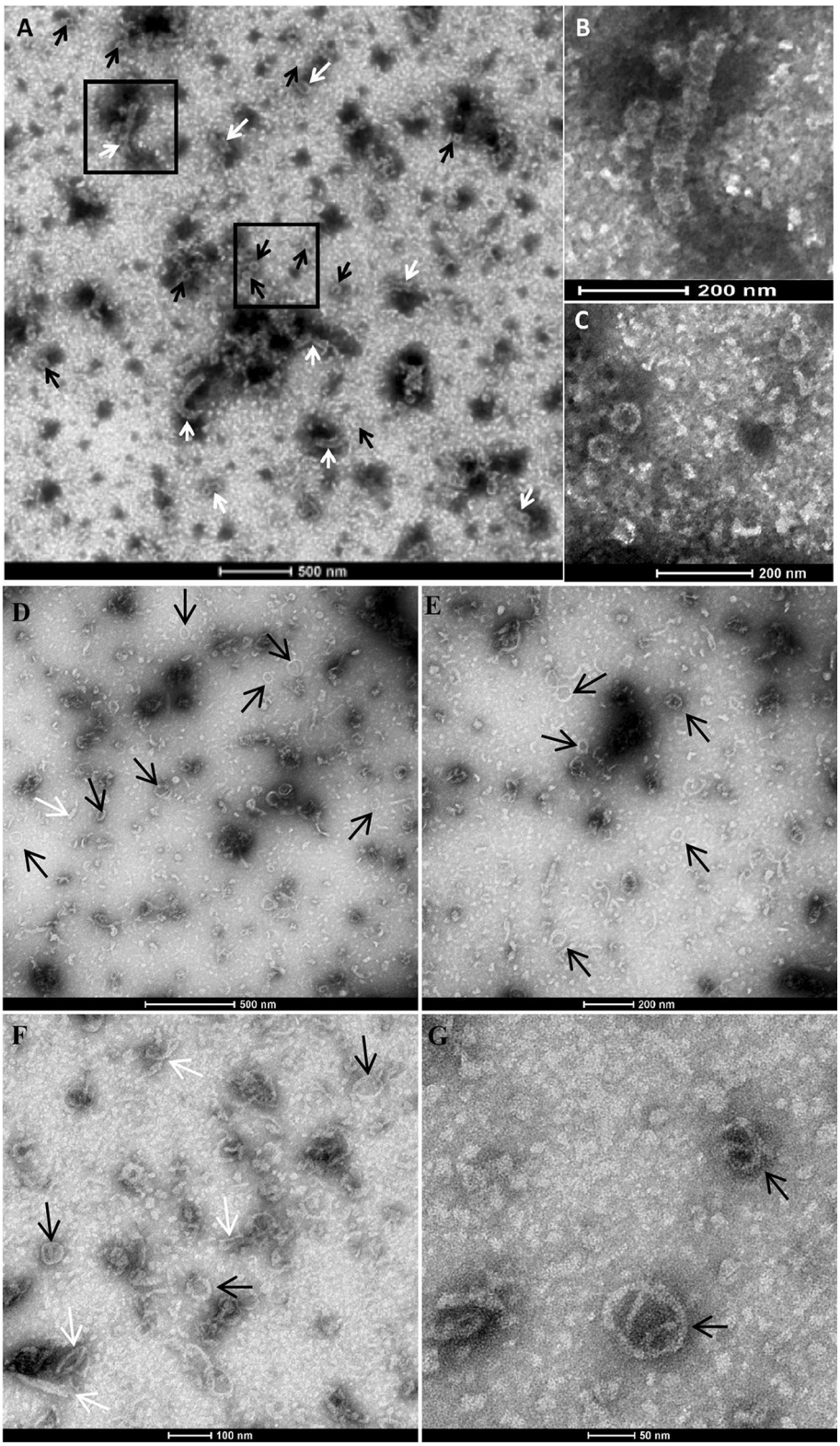

Figure 3. Drp6 forms rings and helical spirals. (**A**–**G**) Electron micrograph of negatively stained Drp6 in the presence of GTPγS. Drp6 (1 μM) at physiological salt concentration in presence of 0.5 mM GTPγS was visualized under electron microscope after negative staining with 2% uranyl acetate. Rings (black arrows) and helical spirals (white arrows) are indicated. The enlarged rings and spirals (boxes in **A**) imaged at higher magnification are shown in (**B**) and (**C**). The scale bar is indicated at the bottom.

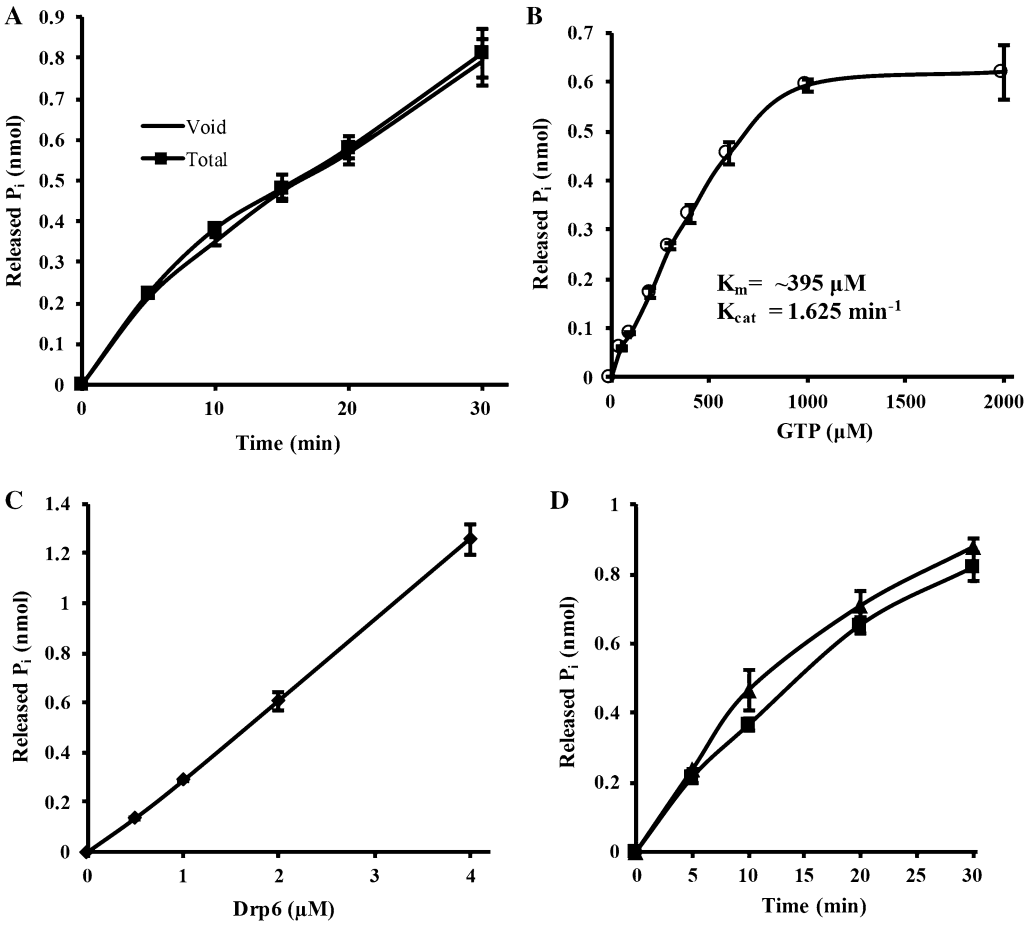

Figure 4. Recombinant Drp6 is catalytically active. (**A**) GTP hydrolysis activity of 1 µM Drp6 with 1mM GTP in buffer B. Total and Void represent Drp6 purified from Ni^{2+}-NTA resin and Drp6 obtained from the void peak of size exclusion chromatography respectively. (**B**) GTP hydrolysis activity using 2 µM Drp6 in buffer B for 10 min. (**C**) GTP hydrolysis activity using 0.5 µM to 4 µM Drp6 with 1 mM GTP in buffer B for 10 min. (**D**) Effect of salt concentration on GTPase activity was analysed by performing assays as in A, either at 150mM NaCl (triangle) or at 40 mM NaCl (square). The amount of P_i released (nmol) was plotted as a function of time (**A** and **D**) or GTP concentration (**B**) or Drp6 concentration (**C**). The plot was generated using Origin Pro 8.0. Statistical significance was calculated with Kruskal–Wallis test (p<0.01) and no significant difference between experiments was observed.

EM experiments were performed in presence of GTPγS, similar self-assembled structures of Drp6 were also observed without adding any nucleotide analog (supplementary figure 5). The formation of such ordered structures at high ionic strength is consistent with the presence of higher order oligomeric species observed in size exclusion chromatography and chemical cross-linking (figure 2).

3.4 *GTPase activity of Drp6*

All dynamin family proteins that have been studied display relatively high basal rates of GTP hydrolysis, and that activity is enhanced by membrane association or by lowering the ionic strength (<50 mM NaCl) (Tuma and Collins 1994; Lin and Gilman 1996; Warnock *et al.* 1996; Prakash *et al.* 2000; Praefcke *et al.* 2004; Gao *et al.* 2010). We assessed the GTP hydrolysis activity of purified Drp6 using a colorimetric assay. Drp6 has high basal GTPase activity with a K_{cat} of ~1.62 min^{-1} and apparent K_m of ~395 µM (figure 4A and B). We measured similar GTPase activities for total purified protein and for a fraction corresponding to the column chromatography void peak (figure 4A), indicating that the high-molecular-weight material does not represent inactive aggregated protein. Moreover, the measured GTPase activity increased linearly with increasing protein concentrations (figure 4C), suggesting that the protein does not tend to form non-specific inactive aggregates.

To ask whether GTPase activity would be enhanced under canonical dynamin assembly conditions, we measured the GTPase activity in low salt condition (<50 mM NaCl). Surprisingly, unlike results for other DRPs we did not

observe any significant change in activity upon lowering the ionic strength of the assay buffer (figure 4D). To rule out that the lack of enhanced GTPase activity of Drp6 is due to the assay conditions used, we have expressed and purified human dynamin 1 in parallel with Drp6 and assessed the GTPase activity under identical conditions. As expected, the GTPase activity of bacterially expressed human dynamin 1 was enhanced more than threefold upon reducing NaCl concentration (<50 mM NaCl) (supplementary figure 6), consistent with earlier report (Kenniston and Lemmon 2010). These findings suggest that unlike canonical dynamin, the GTPase activity of Drp6 is independent of salt concentrations.

4. Discussion

Dynamin-related protein 6 in *Tetrahymena* plays a role in nuclear remodelling (Rahaman *et al.* 2008). As expected for a member of the dynamin family, Drp6 appears to undergo cycles of assembly and disassembly on the nuclear envelope, which are regulated by physiological and developmental cues (Rahaman *et al.* 2008).

In this study, we have analysed biophysical and biochemical properties of Drp6. Specifically, we assessed the oligomeric state, rate of GTP hydrolysis, and ultrastructure, and evaluated the effect of salt concentration on these properties. The bacterially expressed recombinant Drp6 used in this study hydrolyses GTP (figure 4), arguing that the protein is folded in its native structure. Although Drp6 exists mainly as a very-high-molecular-weight structure, size exclusion chromatography also showed the presence of a dimer. Results from size exclusion chromatography and chemical cross-linking clearly demonstrate self-assembly of Drp6 in the absence of any membrane template (figure 2). Since the protein was purified from the supernatant after removing membrane-bound proteins, the higher-order oligomeric structure of Drp6 is not due to its binding to membrane. Drp6 assembled into rings and spirals as visualized by electron micrographs (figure 3 and supplementary figure 4). While similar structures of dynamins and many dynamin-related proteins represent the functional forms, they require lipid binding or low salt condition to form rings and helical spirals (Hinshaw and Schmid 1995; Ramachandran *et al.* 2007; Von Der Malsburg *et al.* 2011; Antonny *et al.* 2016). However, the assembly interface of Drp6 seems to be different from that of dynamins since mutants in the equivalent interface were found to form self-assembled structures. Interestingly, unlike dynamins and other DRPs, MxA exhibits self-assembly property similar to Drp6 where it assembles into rings and helical spirals in the absence of lipid templates (Von Der Malsburg *et al.* 2011). MxA confers antiviral activity by associating with viral nucleoprotein, a function different from canonical membrane remodelling.

Classical dynamin family members, like Dyn1 show cooperative stimulation of GTPase activity upon assembly on lipid templates or at low salt concentrations (<50 mM NaCl) (Muhlberg 1997; Marks *et al.* 2001; Song *et al.* 2004; Antonny *et al.* 2016). In contrast, we did not observe significant enhancement in GTPase activity of Drp6 under low salt concentration (figure 4D). This lack of stimulated GTPase activity is not due to assay conditions since we confirmed stimulation of GTPase activity for Dyn1 under similar conditions. Such lack of stimulation of GTPase activity is also reported for MxA and Drp1 (long iso-form) where assembly onto liposomes did not induce GTP hydrolysis (Von Der Malsburg *et al.* 2011; Macdonald *et al.* 2016). In the case of Drp1, the lack of co-operativity has been attributed to the insertions in the GTPase domain and in the variable domain (Macdonald *et al.* 2016). The plausible explanation for this functional difference between MxA and dynamin is based on arrangement of G-domains in assembled structures (Gao *et al.* 2010; Faelber *et al.* 2011; Von Der Malsburg *et al.* 2011). In case of assembled dynamin, the stimulated GTP hydrolysis is a result of direct contact between the G domains of dynamin protomers in the neighboring turn (Faelber *et al.* 2011; Ford *et al.* 2011). Although dynamin and MxA form similar assembled structures, analysis of Cryo-TEM images revealed that oligomers of MxA are not positioned close enough in the assembled state and hence do not allow inter G domain interactions required for stimulated GTP hydrolysis (Gao *et al.* 2010; Von Der Malsburg *et al.* 2011). It is possible that Drp6 follows a similar arrangement of G domain on target membrane as that of MxA or may have insertional sequences as in case of Drp1, which might explain the lack of enhanced GTPase activity in low ionic strength conditions. However, further studies are required to understand the domain arrangement of Drp6 in self assembled structure and basis of the difference in GTP hydrolysis property as compared to other dynamin family proteins.

Drp6 expressed in bacteria may not be fully active and histidine tag may influence its activity. However, classical endocytic dynamin, when expressed in bacteria as a histidine tag protein, shows activity comparable to that of the native protein (Kenniston and Lemmon 2010). Therefore, we presume that Drp6 expressed similarly represent functional form and conclusion drawn is also relevant for the native protein. Although purified Drp6 catalysed GTP hydrolysis, it could be argued that observed GTPase activity is due to small fraction of functional Drp6 and higher order structure is mainly amorphous aggregates. To exclude this possibility, we have isolated the void peak from gel filtration column and found it to be active. Moreover, increasing protein concentration did not affect GTPase activity (figure 4C) supporting that the GTPase activity obtained is from high-molecular-weight structures and hence they represent functional form of Drp6. Analysis of more than two-hundred

electron micrographs obtained from three independent batches of purified proteins did not show presence of any amorphous aggregates, rather all the micrographs contained self-assembled structures in the form of rings and helical spirals (figure 3 and supplementary figure 4). All these results discussed above confirm that bacterially expressed purified Drp6 used in this study is functional and Drp6 exists as a self-assembled structure as rings and helical spirals without requiring membrane binding.

Drp6 shows differential localization and assembly/disassembly kinetics in *Tetrahymena* and was postulated to be regulated by post-translational modifications (Rahaman *et al.* 2008). The recombinant Drp6 was expressed in bacteria and hence it is expected to lack post-translational modifications. Since the recombinant Drp6 forms self-assembled structure, post-translational modifications do not appear to be essential for assembly into higher order structure. However, it is possible that post-translational modifications regulate the assembly/disassembly dynamics *in vivo*. This would be addressed in future studies.

Although functional significance of target independent self-assembly is not clear, it is postulated that self-assembled structure of human MxA is stored in the cytoplasm and active monomers are released from these stored self-assembled MxA upon viral infection to associate with viral target structure, leading to inhibition of viral replication (Kochs *et al.* 2002). Drp6 localizes both on cytoplasmic puncta and nuclear envelope during vegetative growth of *Tetrahymena*, and has been shown to be essential for macronuclear development (Rahaman *et al.* 2008). It dissociates from nuclear envelope during starvation and early conjugation stages, and re-associates with the nuclear envelope of newly developed nuclei during macronuclear development stage (Rahaman *et al.* 2008). Therefore, it could be proposed that self-assembled structure of Drp6 serves as storage pool and the active lower order oligomeric forms associate with the nuclear envelope during macronuclear development after dissociation from these assembled structures. Alternatively, it is possible that Drp6 is recruited to the target membrane as a self-assembled structure to stabilize membrane curvature change during macronuclear development and subsequently regulates nuclear remodelling. Further studies are required to understand the precise role of membrane independent self-assembly of Drp6 in nuclear remodelling.

Acknowledgements

We thank Prof Aaron Turkewitz from University of Chicago for useful comments on the manuscript. We also thank the TEM facility of MCB, IISc, Bengaluru. This research was supported by funding to AR from the DBT Grant BT/PR14643/BRB/10/862/2010.

References

Antonny B, Burd C, De Camilli P, *et al*. 2016 Membrane fission by dynamin: what we know and what we need to know. *EMBO J.* **35** 2270–2284

Carr JF and Hinshaw JE 1997 Dynamin assembles into spirals under physiological salt conditions upon the addition of GDP and gamma-phosphate analogues. *J. Biol. Chem*. **272** 28030–28035

Chan DC 2006 Mitochondrial fusion and fission in mammals. *Annu. Rev. Cell Dev. Biol*. **22** 79–99

Chang CR and Blackstone C 2010 Dynamic regulation of mitochondrial fission through modification of the dynamin-related protein Drp1. *Ann. NY Acad. Sci*. **1201** 34–39

Chang CR, Manlandro CM, Arnoult D, *et al.* 2010 A lethal de novo mutation in the middle domain of the dynamin-related GTPase Drp1 impairs higher order assembly and mitochondrial division. *J. Biol. Chem*. **285** 32494–32503

Chen Y-J, Zhang P, Egelman EH and Hinshaw JE 2004 The stalk region of dynamin drives the constriction of dynamin tubes. *Nat. Struct. Mol. Biol*. **11** 574–575

Cocucci E, Gaudin R and Kirchhausen T 2014 Dynamin recruitment and membrane scission at the neck of a clathrin-coated pit. *Mol. Biol. Cell* **25** 3595–3609

Faelber K, Held M, Gao S, *et al.* 2012 Structural insights into dynamin-mediated membrane fission. *Structure* **20** 1621–1628

Faelber K, Posor Y, Gao S, *et al.* 2011 Crystal structure of nucleotide-free dynamin. *Nature* **477** 556–560

Ford MGJ, Jenni S and Nunnari J 2011 The crystal structure of dynamin. *Nature* **477** 561–566

Fritz S, Rapaport D, Klanner E, *et al*. 2001 Connection of the mitochondrial outer and inner membranes by Fzo1 is critical for organellar fusion. *J. Cell Biol*. **152** 683–692

Gao S, von der Malsburg A, Paeschke S, *et al.* 2010 Structural basis of oligomerization in the stalk region of dynamin-like MxA. *Nature* **465** 502–506

Haller O and Kochs G 2011 Human MxA protein: an interferon-induced dynamin-like GTPase with broad antiviral activity. *J. Interf. Cytokine Res.* **31** 79–87

Haller O, Stertz S and Kochs G 2007 The Mx GTPase family of interferon-induced antiviral proteins. *Microbe. Infect*. **9** 1636–1643

Hermann GJ, Thatcher JW, Mills JP, *et al*. 1998 Mitochondrial fusion in yeast requires the transmembrane GTPase Fzo1p. *J. Cell Biol*. **143** 359–373

Hinshaw JE 2000 Dynamin and its role in membrane fission. *Annu. Rev. Cell Dev. Biol.* **16** 483–519

Hinshaw JE and Schmid SL 1995 Dynamin self-assembles into rings suggesting a mechanism for coated vesicle budding. *Nature* **374** 190–192

Kar UP, Dey H and Rahaman A 2017 Regulation of dynamin family proteins by post-translational modifications. *J. Biosci.* **42** 333–344

Kenniston JA and Lemmon MA 2010 Dynamin GTPase regulation is altered by PH domain mutations found in centronuclear myopathy patients. *EMBO J.* **29** 3054–3067

Kochs G, Haener M, Aebi U and Haller O 2002 Self-assembly of human MxA GTPase into highly ordered dynamin-like oligomers. https://doi.org/10.1074/jbc.M200244200

Lin HC and Gilman AG 1996 Regulation of dynamin I GTPase activity by G protein subunits and phosphatidylinositol 4,5-bisphosphate. *J. Biol. Chem*. **271** 27979–27982

Low HH, Sachse C, Amos LA and Löwe J 2009 Structure of a bacterial dynamin-like protein lipid tube provides a mechanism for assembly and membrane curving. *Cell* **139** 1342–1352

Macdonald PJ, Francy CA and Stepanyants N, *et al.* 2016 Distinct Splice variants of dynamin-related protein 1 differentially utilize mitochondrial fission factor as an effector of cooperative GTPase activity. *J. Biol. Chem*. **291** 493–507

Marks B, Stowell MH, Vallis Y, *et al.* 2001 GTPase activity of dynamin and resulting conformation change are essential for endocytosis. *Nature* **410** 231–235

Mears JA, Lackner LL, Fang S, *et al.* 2011 Conformational changes in Dnm1 support a contractile mechanism for mitochondrial fission. *Nat. Struct. Mol. Biol.* **18** 20–26

Meglei G and McQuibban GA 2009 The dynamin-related protein Mgm1p assembles into oligomers and hydrolyzes GTP to function in mitochondrial membrane fusion. *Biochemistry* **48** 1774–1784

Moss TJ, Andreazza C, Verma A, *et al.* 2011 Membrane fusion by the GTPase atlastin requires a conserved C-terminal cytoplasmic tail and dimerization through the middle domain. *Proc. Natl. Acad. Sci. USA* **108** 11133–11138

Muhlberg AB 1997 Domain structure and intramolecular regulation of dynamin GTPase. *EMBO J.* **16** 6676–6683

Praefcke GJ, Kloep S, Benscheid U, *et al.* 2004 Identification of residues in the human guanylate-binding protein 1 critical for nucleotide binding and cooperative GTP hydrolysis. *J. Mol. Biol.* **344** 257–269

Praefcke GJK and McMahon HT 2004 The dynamin superfamily: universal membrane tubulation and fission molecules? *Nat. Rev. Mol. Cell Biol*. **5** 133–147

Prakash B, Praefcke GJK, Renault L, *et al.* 2000 Structure of human guanylate-binding protein 1 representing a unique class of GTP-binding proteins. *Nature* **403** 567–571

Rahaman A, Elde NC and Turkewitz AP 2008 A dynamin-related protein required for nuclear remodeling in Tetrahymena. *Curr. Biol.* **18** 1227–1233

Ramachandran R, Surka M, Chappie JS, *et al.* 2007 The dynamin middle domain is critical for tetramerization and higher-order self-assembly. *EMBO J.* **26** 559–566

Richter MF, Schwemmle M, Herrmann C, *et al.* 1995 Interferon-induced MxA protein. GTP binding and GTP hydrolysis properties. *J. Biol. Chem*. 270 13512–13517

Sesaki H, Southard SM, Yaffe MP and Jensen RE 2003 Mgm1p, a dynamin-related {GTPase,} is essential for fusion of the mitochondrial outer membrane. *Mol. Biol. Cell* **14** 2342–2356

Song BD, Yarar D and Schmid SL 2004 An assembly-incompetent mutant establishes a requirement for dynamin self-assembly in clathrin- mediated endocytosis in vivo. *Mol. Biol. Cell* **15** 2243–2252

Sweitzer SM and Hinshaw JE 1998 Dynamin undergoes a GTP-dependent conformational change causing vesiculation. *Cell* **93** 1021–1029

Tadato B, Heymann JAW, Song Z, *et al.* 2010 OPA1 disease alleles causing dominant optic atrophy have defects in cardiolipin-stimulated GTP hydrolysis and membrane tubulation. *Hum. Mol. Genet*. **19** 2113–2122

Takei K, McPherson PS, Schmid SL and De Camilli P 1995 Tubular membrane invaginations coated by dynamin rings are induced by GTP-gamma S in nerve terminals. *Nature* **374** 186–190

Tuma PL and Collins CA 1994 Activation of dynamin GTPase is a result of positive cooperativity. *J. Biol. Chem.* **269** 30842–30847

van der Bliek AM, Shen Q and Kawajiri S 2013 Mechanisms of mitochondrial fission and fusion. *Cold Spring Harb. Perspect. Biol*. https://doi.org/10.1101/cshperspect.a011072

Von Der Malsburg A, Abutbul-Ionita I, Haller O, *et al.* 2011 Stalk domain of the dynamin-like MxA GTPase protein mediates membrane binding and liposome tubulation via the unstructured L4 loop. *J. Biol. Chem.* **286** 37858–37865

Warnock DE, Hinshaw JE and Schmid SL 1996 Dynamin self-assembly stimulates its GTPase activity. *J. Biol. Chem*. **271** 22310–22314

Yoon Y, Pitts KR and McNiven MA 2001 Mammalian dynamin-like protein DLP1 tubulates membranes. *Mol. Biol. Cell* **12** 2894–2905

Zhu PP, Patterson A, Stadler J, *et al.* 2004 Intra- and intermolecular domain interactions of the C-terminal GTPase effector domain of the multimeric dynamin-like GTPase Drp1. *J. Biol. Chem*. **279** 35 967–35974

Corresponding editor: Ullas Kolthur Seetharam